

Analysis of the Heterogeneous Vectorial Network Model of Collective Motion

Jalil Hasanyan, Lorenzo Zino, Agnieszka Truszkowska, Alessandro Rizzo, Maurizio Porfiri

Abstract—We analyze the vectorial network model, a stochastic protocol that describes the collective dynamics of groups of self-propelled agents that randomly mix in a planar space. Motivated by biological and technical applications, we focus on a heterogeneous form of the model, where agents have different propensities to interact with others. By linearizing the dynamics about a synchronous state and leveraging an eigenvalue perturbation argument, we establish a closed-form expression for the mean-square convergence rate to the synchronous state in the absence of additive noise. These closed-form findings are extended to study the effect of added noise on the agents' coordination, captured by the polarization of the group. Our results reveal that heterogeneity has a detrimental effect on both the convergence rate and the polarization, which is nonlinearly moderated by the average number of connections in the group. Numerical simulations are provided to support our theoretical findings.

I. INTRODUCTION

Collective motion is a widely studied phenomenon across biology, physics, and engineering [1], [2], [3]. The emergence of collective motion is often observed in animal groups, such as bird flocks, fish schools, and sheep herds. Social animals have been shown to use locally controlled interactions for decision-making that ultimately regulate their motion and coordination [1]. To mimic these dynamics and better understand the emergence of coordination, the physics community has established a wide range of mathematical models of collective motion for groups of self-propelled particles [2]. In the engineering community, the observations on the spontaneous emergence of coordination in biological systems and the mathematical models developed in the physics community have inspired the design and analysis of decentralized control schemes for groups of autonomous robots [3].

The vectorial network model (VNM), originally proposed by [4], [5], has emerged as a valuable paradigm to describe collective motion for its mathematical tractability and ability to reproduce important features of more complex models.

J. Hasanyan, A. Truszkowska, and M. Porfiri are with the Department of Mechanical and Aerospace Engineering, New York University Tandon School of Engineering, Brooklyn, New York 11201, USA. L. Zino is with the Faculty of Science and Engineering, ENTEG, University of Groningen, Groningen 9747 AG, Netherlands. A. Rizzo is with the Department of Electronics and Telecommunications, Politecnico di Torino, Torino, Italy. He is also with the Office of Innovation, New York University Tandon School of Engineering, Brooklyn NY 11201, USA. M. Porfiri is also the Department of Biomedical Engineering, New York University Tandon School of Engineering, Brooklyn NY 11201, USA (mporfiri@nyu.edu).

This work was partially supported by the National Science Foundation (CMMI-1561134), Mitsui-USA Fundation, Compagnia di San Paolo, MAECl (“Mac2Mic”), European Research Council (ERC-CoG-771687), and Netherlands Organization for Scientific Research (NWO-vidi-14134).

In the VNM, each agent is characterized by its orientation on a planar space. Agents interact through a stochastically switching network, through which they dynamically update their orientation to synchronize with their neighbors. Such a dynamic updating is affected by intrinsic noise. The VNM has been initially proposed as a proxy of the classical Vicsek model [6], whose complexity restricted its analysis to numerical simulations [7], [8], [9], [10] or case-specific theoretical results [11], [12], [13], [14], [15].

The first analyses of the VNM were performed in the thermodynamic limit of large-scale systems, through extensive numerical simulations [4] and semi-analytical approaches [5]. These studies demonstrated the existence of a continuous order-disorder phase transition, similar to the Vicsek model in the case of rapidly moving particles that randomly mix at every time step [6]. For small values of added noise, the agents are successful in coordinating their motion. The extent of such a coordination smoothly decreases as the noise increases, until reaching completely disordered states when the level of noise is above a critical value. Further insight into the nature of the phase transition and its dependence on system parameters can be found in [16], where a mean-field theory of the VNM is developed and analytically investigated.

In [17], the VNM is analyzed without relying on the thermodynamic limit, via a linearization process that allows the VNM to be studied through the lens of consensus protocols [18], [19], specifically, stochastic protocols with additive noise [20]. This linear analysis begot an array of closed-form results for homogeneous groups of agents, that is, where agents are indistinguishable in their ability to form connections with other group members. These results helped elucidate the effect of the population size, the number of connections of each agent, and noise on the coordination of the VNM. Further studies on the linearized VNM have shed light on various aspects of the collective dynamics, such as the effect of leader-follower interactions [21] and of specific choices of the noise inspired by biological applications [22].

All these analyses are based on the assumption that all the agents interact with the same number of individuals. Such an assumption is not reflective on many real-life complex systems. For instance, heterogeneity between the members of a group is a typical feature of animal groups [23] and complex coordination schemes between autonomous robots often involve the cooperation of different models or generations of robots [24]. Heterogeneity, indeed, has been shown to play a key, nontrivial role in many coordination processes. On the one hand, heterogeneous distribution of

network connectivity hinders network synchronization in small-world networks [25] and convergence of stochastic consensus protocols [26]. On the other hand, the emergence of ordered states in complex networks may be favored by heterogeneous coupling [27] and convergence of stochastic consensus protocols, in the presence of leader-follower interactions, may instead be helped by heterogeneity [28]. To the best of our knowledge, there is still a gap in the theoretical understanding of the role of heterogeneity in the VNM. Filling this gap is expected to bring insight into collective motion of more complex models, thereby informing the design of coordination strategies for engineering systems and the understanding of real-life complex systems.

To this end, we examine the VNM in the general case where each agent is characterized by a different propensity to form connections with other group members. Similar to [17], we rely on a linearization of the VNM about a synchronous state, and we present a toolbox of analytical results that capture the effect of heterogeneity on the asymptotic behavior of the VNM. First, through stochastic stability theory and eigenvalue perturbation methods, we establish closed-form results for the asymptotic convergence factor, which determines the convergence rate in the absence of noise. Our findings suggest that convergence to synchronous states is hindered by the heterogeneity of the agents' attitude to interact with others, at least for moderate levels of heterogeneity. In agreement with our intuition, this detrimental effect is moderated by the number of connections, where synchronization in denser networks is more robust to the effect of heterogeneity. Second, we study the polarization of the system [4], which is a global observable that quantifies the level of coordination between the agents. Following [17] and leveraging a perturbation argument, we derive a closed-form approximation for the polarization, which is exact in the small noise limit. Such an expression corroborates our previous finding, confirming that heterogeneity is detrimental for the emergence of ordered states, not only by slowing down the convergence, but also by decreasing the level of coordination of the system. Monte Carlo numerical simulations are provided to validate our analytical findings.

II. PROBLEM STATEMENT

A. Notation

The set of real numbers and nonnegative integers are represented by \mathbb{R} and \mathbb{Z}^+ , respectively. Given a vector \mathbf{x} , we denote its transpose by \mathbf{x}^\top . The N -dimensional all-1 (or 0) vector is denoted as $\mathbf{1}$ (or $\mathbf{0}$), and the N -dimensional identity matrix by \mathbf{I} . The Euclidean norm of a vector is indicated by $\|\cdot\|$, the vectorization of a matrix by $\text{vec}(\cdot)$, the argument of a complex number by $\text{Angle}\{\cdot\}$, the expectation and the variance of a random variable by $\mathbb{E}[\cdot]$ and $\text{var}[\cdot]$, respectively. Matrix operations denoted by \otimes and \oslash are the Kronecker product and the Hadamard division, respectively. The spectral radius of a matrix is indicated by $\rho(\cdot)$.

B. Heterogeneous VNM

We consider a system of N agents. Agent $i \in \{1, \dots, N\}$ is associated with the two-dimensional, unit-length vector $v_i = e^{i\theta_i}$ with i being the imaginary unit. With reference to the Vicsek model [6], the vector represents the heading direction of the self-propelled particle. Each vector v_i updates its orientation θ_i according to a discrete-time process, as a consequence of interactions with other vectors. Agents are heterogeneous in their attitude to interact with others. Specifically, each agent i is characterized by a constant $a_i \in \mathbb{Z}^+$ that measures the number of interactions that i establishes at each time-step. These constants are gathered in the *interaction vector* \mathbf{a} . Similar to [26], we express the interaction vector as $\mathbf{a} = K\mathbf{1} + \sigma\mathbf{h}$, where

$$K := \frac{1}{N} \sum_{i=1}^N a_i \quad \text{and} \quad \sigma := \sqrt{\frac{1}{N} \sum_{i=1}^N (a_i - K)^2}, \quad (1)$$

are the average number of interactions and its standard deviation, respectively. Vector $\mathbf{h} \in \mathbb{R}^N$ captures the deviations from the average number of connections and is such that $\mathbf{1}^\top \mathbf{h} = 0$, and $\|\mathbf{h}\| = \sqrt{N}$. In the original formulation of the VNM [4], [5], agents have homogeneous propensities of interaction, that is, for $a_i = K$, for $i = 1, \dots, N$.

At each time-step $k \in \mathbb{Z}^+$, agent i is connected with a_i agents, $\{i1, \dots, ia_i\}$, whose average vector is

$$U_i(k) = \frac{1}{a_i} \sum_{p=1}^{a_i} v_{ip}(k). \quad (2)$$

This vector is used as input to update the orientation of agent i according to the following stochastic dynamics:

$$\theta_i(k+1) = \text{Angle}\{U_i(k)\} + \eta \zeta_i(k), \quad (3)$$

where the constant $\eta \in [0, 1]$ is the noise intensity and $\zeta_i(k)$ is a sequence of independent and identically distributed (i.i.d.) random variables drawn from a uniform distribution in $[-\pi, \pi]$.

III. PRELIMINARIES

A. Linearization of the VNM

We begin our analysis by linearizing Eq. (3) with respect to the orientation around a synchronous state, θ_0 , where $\theta_i(k) = \theta_0 + x_i(k)$, to obtain

$$x(k+1) = W(k)x(k) + \eta \zeta_i(k), \quad (4)$$

where $x(k) = [x_1(k) \ \dots \ x_n(k)]^\top \in \mathbb{R}^N$ is the state vector, $\zeta(k) = [\zeta_1(k) \ \dots \ \zeta_n(k)]^\top \in \mathbb{R}^N$ is the additive noise, and $W(k) \in \mathbb{R}^{N \times N}$ is the state matrix. Matrices $W(k)$'s are a sequence of i.i.d. random variables with common random variables W . The matrix W is defined row-wise as follows. Row i of W is the sum of a_i i.i.d. vectors V_{i1}, \dots, V_{ia_i} , with all entries equal to 0, except one entry equal to $\frac{1}{a_i}$, selected

uniformly at random. That is,

$$W = \begin{bmatrix} \sum_{p=1}^{a_i} V_{1p}^\top \\ \vdots \\ \sum_{p=1}^{a_i} V_{Np}^\top \end{bmatrix}. \quad (5)$$

Hence, it is straightforward to check that: i) $\mathbb{E}[W_{ij}] = \frac{1}{N}$, for all $i, j \in \{1, \dots, N\}$, and ii) W is row-stochastic, that is, $W\mathbf{1} = \mathbf{1}$.

B. Asymptotic behavior

The linearized heterogeneous VNM is studied through the disagreement dynamics of Eq. (4), that is, $\xi(k) = x(k) - \bar{x}(k)\mathbf{1}$, where $\bar{x}(k) = \frac{1}{N}\mathbf{1}^\top x(k)$ is the average state. The evolution of the disagreement dynamics is given by

$$\xi(k+1) = RW(k)\xi(k) + \eta R\zeta_i(k), \quad (6)$$

where $R = I - \frac{1}{N}\mathbf{1}\mathbf{1}^\top$ projects \mathbb{R}^N onto the subspace orthogonal to $\mathbf{1}$.

Based on previous work [17], [29], [30], we study the evolution of the disagreement dynamics in a mean-square sense. Specifically, we examine the time evolution of the autocorrelation matrix $\Xi(k) = \mathbb{E}[\xi(k)\xi(k)^\top]$. Recalling that ζ and W are i.i.d. random variables, that $\mathbb{E}[\zeta] = \mathbf{0}$, and that $\mathbb{E}[\zeta\zeta^\top] = \frac{\pi^2}{3}I$, we compute

$$\begin{aligned} \text{vec}(\Xi(k+1)) &= \\ &= G^k \text{vec}(\xi(0)\xi(0)^\top) + \eta^2 \left(\sum_{i=0}^{k-1} G^i \right) R \otimes R \text{vec}(\mathbb{E}[\zeta\zeta^\top]) \\ &= G^k \text{vec}(\xi(0)\xi(0)^\top) + \eta^2 \frac{\pi^2}{3} \left(\sum_{i=0}^{k-1} G^i \right) \text{vec}(R), \end{aligned} \quad (7)$$

with

$$G = R \otimes R \mathbb{E}[W \otimes W]. \quad (8)$$

From Eq. (7), we observe that the time evolution of the autocorrelation is fully determined by matrix G . In the absence of noise (that is, $\eta = 0$), the mean-square asymptotic behavior of Eq. (6) is determined by the spectral radius of G , which is called the *asymptotic convergence factor* r [31], [32]. If $r < 1$, then the autocorrelation in Eq. (7) converges to a finite value as $k \rightarrow \infty$, yielding

$$\text{vec}(\Xi_\infty) = \eta^2 (I \otimes I - G)^{-1} \text{vec}(R). \quad (9)$$

The trace of Ξ_∞ is called the mean-square deviation and it corresponds to the limit of $\mathbb{E}[||\xi(k)||^2]$, which is equal to

$$\delta_\infty = \eta^2 \text{vec}(R) (I \otimes I - G)^{-1} \text{vec}(R). \quad (10)$$

C. Order parameter

The coordination of the agents is quantified by means of a global observable called *polarization* [4], [5], which is defined as

$$\text{Pol} := \lim_{k \rightarrow \infty} \mathbb{E} \left[\frac{1}{N} \left| \sum_{i=1}^N \exp(\iota\theta_i(k)) \right| \right], \quad (11)$$

whereby $\text{Pol} = 0$ indicates a completely disordered state, while $\text{Pol} = 1$ indicates full alignment of the agents' orientations.

We use the mean-square steady state deviation to approximate the polarization for small levels of noise $\eta \ll 1$, following the analysis of the homogeneous VNM in [17]. To this end, we introduce a linear approximation of the heading, $\theta_i(k) = \theta_0 + x_i(k)$, for $i = 1, \dots, N$, and expand up to the second order to find

$$\text{Pol} \approx 1 - \frac{1}{2N} \delta_\infty. \quad (12)$$

IV. MAIN RESULTS

Here, we analyze the linearized heterogeneous VNM, establishing closed-form expressions for the spectral radius $\rho(G)$ and the mean-square deviation δ_∞ , which determine the convergence rate and the degree of coordination, respectively. We begin by deriving the closed-form expression of matrix G in Eq. (8) as a function of the interaction vector \mathbf{a} . Our result is summarized in the following proposition.

Proposition 1. *The matrix G in Eq. (8) associated with the linearized heterogeneous VNM in Eq. (4) with interaction vector \mathbf{a} is equal to*

$$G = R \otimes R \mathbb{E}[W \otimes W] = \frac{1}{N} \text{vec}(R \text{diag}(\mathbf{1} \otimes \mathbf{a}) R) \text{vec}(R)^\top. \quad (13)$$

Proof. We use a counting argument, similar to [17]. Due to the structure of the Kronecker product, the matrix $\mathbb{E}[W \otimes W]$ has a block structure and its entries are in the form $\mathbb{E}[W_{ij}W_{st}]$, for $i, j, s, t = 1, \dots, N$. Using Eq. (5), we observe that these entries can have three different expressions, depending on their indexes: i) for $i = s$ and $j = t$,

$$\begin{aligned} \mathbb{E}[W_{ij}^2] &= \mathbb{E} \left[\left(\sum_{p=1}^{a_i} (V_{ip})_j \right)^2 \right] = \text{var} \left[\sum_{p=1}^{a_i} (V_{ip})_j \right] \\ &+ \mathbb{E} \left[\sum_{p=1}^{a_i} (V_{ip})_j \right]^2 = \frac{N-1}{N^2 a_i} + \frac{1}{N^2} = \frac{N+a_i-1}{N^2 a_i}; \end{aligned}$$

ii) for $i = s$ and $j \neq t$, we compute

$$\begin{aligned} \mathbb{E}[W_{ij}W_{st}] &= \sum_{p=1}^{a_i} \sum_{q=1}^{a_s} \mathbb{E}[(V_{ip})_j (V_{iq})_t] \\ &= \sum_{p=1}^{a_i} \sum_{\substack{q=1, q \neq p}}^{a_s} \mathbb{E}[(V_{ip})_j] \mathbb{E}[(V_{iq})_t] = \frac{a_i-1}{N^2 a_i}; \end{aligned}$$

and, iii) for $i \neq s$, we use the independence between the rows of W to conclude

$$\mathbb{E}[W_{ij}W_{st}] = \mathbb{E}[W_{ij}]\mathbb{E}[W_{st}] = \frac{1}{N^2}.$$

Thus, we find

$$\begin{aligned} \mathbb{E}[W \otimes W] &= \frac{1}{N} \text{vec}(\text{diag}(\mathbf{1} \otimes \mathbf{a})) \text{vec}(R)^\top \\ &+ \frac{1}{N^2} \mathbf{1}\mathbf{1}^\top \otimes \mathbf{1}\mathbf{1}^\top. \end{aligned}$$

Finally, the premultiplication by $R \otimes R$ yields Eq. (13). \square

A. Convergence rate in the absence of noise

The nontrivial structure of matrix G for the heterogeneous VNM in Eq. (13) hinders the direct computation of its spectral radius. To overcome this issue, we pursue a perturbation argument with respect to σ . Using the expression $a_i = K + \sigma h_i$, we write the matrix G in Eq. (13) as

$$G = G_0 + \sigma G_1 + \sigma^2 G_2 + O(\sigma^3) \quad (14)$$

where

$$G_0 = \frac{1}{KN} \text{vec}(R) \text{vec}(R)^\top, \quad (15a)$$

$$G_1 = -\frac{1}{K^2 N} \text{vec}(R \text{diag}(\mathbf{h}) R) \text{vec}(R)^\top, \text{ and} \quad (15b)$$

$$G_2 = \frac{1}{K^3 N} \text{vec}(R \text{diag}(\mathbf{h}^2) R) \text{vec}(R)^\top, \quad (15c)$$

where \mathbf{h}^2 is meant entry-wise. For $\sigma = 0$, the VNM reduces to the homogeneous scenario with $G = G_0$ studied in [17], in which all agents establish K interactions at each time-step. The simple structure of G_0 (which is a symmetric rank-1 matrix) allows to fully determine its spectrum, as summarized in the following.

Lemma 1. *The spectral radius of G_0 is $\rho_0 = \frac{N-1}{KN}$, with associated unit-length eigenvector $u_0 = \frac{1}{\sqrt{N-1}} \text{vec}(R)$. All the other eigenvalues are zero, that is, $\lambda_2 = \dots = \lambda_{N^2} = 0$.*

This implies that the rate of convergence in the homogeneous VNM improves monotonically as the number of interactions K grows. To elucidate the effect of heterogeneity, we recall a classical result on second-order perturbation theory of simple eigenvalues, which is used to derive our second-order approximation of the spectral radius $\rho(G)$.

Proposition 2 ([33], Chapter 6). *Given a matrix G in the form Eq. (14), if the spectral radius $\rho_0 = \rho(G_0)$ is a simple eigenvalue of G_0 , then the spectral radius of G can be expressed as*

$$\rho(G) = \rho_0 + \sigma \rho_1 + \sigma^2 \rho_2 + O(\sigma^3). \quad (16)$$

The perturbation terms are equal to

$$\rho_1 = u_0^\top G_1 u_0 \quad \text{and} \quad \rho_2 = u_0^\top G_1 u_1 + u_0^\top G_2 u_0, \quad (17)$$

with $u_0 = \frac{1}{\sqrt{N-1}} \text{vec}(R)$ and

$$u_1 = \sum_{i=2}^{N^2} \frac{v_i^\top G_1 u_0}{\rho_0 - \lambda_i} v_i, \quad (18)$$

where $\lambda_2, \dots, \lambda_{N^2}$ are the $N^2 - 1$ eigenvalues of matrix G_0 different from ρ_0 , and v_2, \dots, v_{N^2} are their corresponding unit-norm eigenvectors.

Theorem 1. *The spectral radius of the matrix G in Eq. (13) of a VNM with interaction vector \mathbf{a} is equal to*

$$\rho(G) = \frac{N-1}{KN} + \sigma^2 \frac{N-1}{K^3 N} + O(\sigma^3). \quad (19)$$

Proof. We observe that the following equalities hold: i) $\text{vec}(R)^\top G_1 = \mathbf{0}$, and ii) $\text{vec}(R)^\top \text{vec}(R \text{diag}(\mathbf{h}^2) R) =$

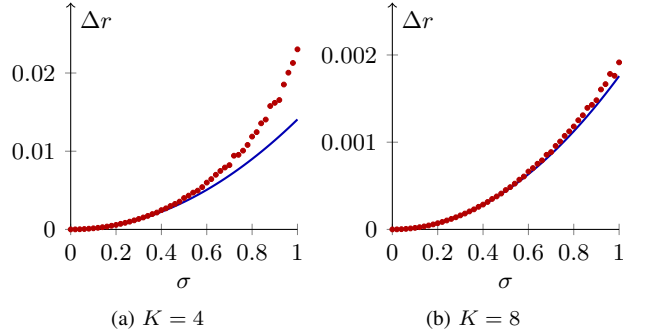


Fig. 1: Variation of the spectral radius of G with respect to the one for the homogeneous VNM, $\Delta r = \rho(G) - \rho_0$, for different levels of heterogeneity σ . The blue solid curves are the analytical predictions, computed according to the second-order perturbation in Eq. (17); the red circles are Monte Carlo numerical estimation of the spectral radius of Eq. (8) over 100 independent realizations of the vector \mathbf{h} , generated randomly such that $\mathbf{1}^\top \mathbf{h} = 0$ and $\|\mathbf{h}\| = \sqrt{N}$. In both panels $N = 10$; in (a) $K = 4$, in (b) $K = 8$.

$N - 1$. From i), we conclude that the first-order perturbation $\rho_1 = u_0^\top G_1 u_0 = 0$, and the first summand of ρ_2 in Eq. (17) $u_0^\top G_1 u_1 = 0$. Using ii), we compute the second summand in the expression of ρ_2 in Eq. (17), which yields the claim. \square

Remark 1. *For $\sigma = 0$, the expression in Eq. (19) reduces to $\rho(G) = \frac{N-1}{KN}$, as observed in [17]. In the presence of heterogeneity, the asymptotic convergence factor increases, hindering mean-square convergence. Specifically, we find that the increase in the spectral radius of G caused by heterogeneity increases proportionally to the square of the standard deviation of the interaction vector σ , while it decreases as the average number of interactions K increases, being inversely proportional to the cube of K .*

The comparison between our analytical approximation and numerical computations of the spectral radius illustrated in Fig. 1 supports the theoretical findings in Theorem 1 and suggests that the second-order approximation derived in Eq. (19) provides an accurate estimate of the spectral radius of the matrix G up to moderate levels of heterogeneity σ . The accuracy of the approximation seems to increase with the average number of interactions K .

B. Coordination in the presence of noise

Here, we put forward a similar perturbation argument on the matrix G to derive a second-order approximation of the mean-square deviation δ_∞ in Eq. (10), which allows to approximate the polarization as in Eq. (12). The results of our analysis are summarized in the following theorem.

Theorem 2. *The mean-square deviation δ_∞ in Eq. (10) of the heterogeneous VNM with interaction vector \mathbf{a} in Eq. (12)*

is equal to

$$\begin{aligned}\delta_\infty &= \eta^2 \frac{\pi^2}{3} \frac{KN(N-1)}{N(K-1)+1} \\ &+ \sigma^2 \eta^2 \frac{\pi^2}{3} \frac{N(N-1)^2}{K(N(K-1)+1)^2} + O(\sigma^3).\end{aligned}\quad (20)$$

Proof. We write the term $(I \otimes I - G)^{-1}$ in Eq. (10) as a power series and we expand G using Eq. (14), obtaining

$$\begin{aligned}(I \otimes I - G)^{-1} &= I \otimes I + \sum_{n=1}^{\infty} G^n \\ &= I \otimes I + \sum_{n=1}^{\infty} G_0^n + \sigma \sum_{n=1}^{\infty} \sum_{\ell=0}^{n-1} G_0^\ell G_1 G_0^{n-\ell-1} \\ &+ \sigma^2 \sum_{n=1}^{\infty} \sum_{\ell=0}^{n-1} G_0^\ell G_2 G_0^{n-\ell-1} \\ &+ \sigma^2 \sum_{n=2}^{\infty} \sum_{\ell=0}^{n-2} \sum_{m=0}^{n-\ell-2} G_0^\ell G_1 G_0^m G_1 G_0^{n-\ell-m-2} + O(\sigma^3).\end{aligned}\quad (21)$$

From the expressions of G_0 , G_1 , and G_2 in Eq. (15), we observe that $G_0 G_1 = G_1 G_0 = G_1^2 = 0_{N \times N}$. Hence, the third and the fifth terms in Eq. (21) are equal to 0. We substitute the remaining terms of Eq. (21) into Eq. (10), obtaining three contributions to the expression of δ_∞ , up to the $O(\sigma^3)$ term. Specifically, we have two zeroth-order terms and one second-order term in σ , coming from the first, second, and fourth summands in Eq. (21), respectively. The first two terms yield the mean-square deviations for an homogeneous VNM with K interactions, which is equal to $\eta^2 \frac{\pi^2}{3} \frac{KN(N-1)}{N(K-1)+1}$, as computed in [17]. Finally, we compute

$$\begin{aligned}&\eta^2 \frac{\pi^2}{3} \text{vec}(R)^\top \left(\sigma^2 \sum_{n=1}^{\infty} \sum_{\ell=0}^{n-1} G_0^\ell G_2 G_0^{n-\ell-1} \right) \text{vec}(R) \\ &= \eta^2 \frac{\pi^2}{3} \sigma^2 \sum_{n=1}^{\infty} \sum_{\ell=0}^{n-1} \left(\frac{N-1}{NK} \right)^{n-1} \text{vec}(R)^\top G_2 \text{vec}(R) \\ &= \eta^2 \frac{\pi^2}{3} \sigma^2 \sum_{n=1}^{\infty} n \left(\frac{N-1}{NK} \right)^{n-1} \frac{(N-1)^2}{NK^3} \\ &= \eta^2 \frac{\pi^2}{3} \frac{(N-1)^2}{NK^3} \sigma^2 \frac{1}{(1 - \frac{N-1}{NK})^2} \\ &= \eta^2 \frac{\pi^2}{3} \sigma^2 \frac{N(N-1)^2}{K(N(K-1)+1)^2}.\end{aligned}$$

□

Remark 2. From Eq. (20), one can compute an approximation of the polarization in Eq. (12) that is valid for small added noise. For $\sigma = 0$, this expression reduces to the one computed by [17] for the homogeneous VNM; for $\sigma > 0$, the polarization decreases, such that the presence of heterogeneity hinders coordination.

We compare the closed-form expression for the polarization based on Eq. (12) and Eq. (20), with Monte Carlo estimations of Eq. (11), computed by numerically simulating the nonlinear VNM. Simulations are conducted for $N = 80$ agents, initialized at $\theta_i(0) = 0$, for $i = 1, \dots, N$. For

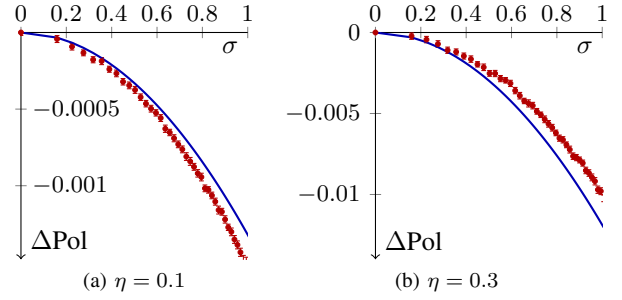


Fig. 2: Variation of the polarization with respect to the homogeneous VNM, $\Delta\text{Pol} = \text{Pol} - \text{Pol}_0$, where Pol_0 is the polarization of the homogeneous VNM, for different levels of heterogeneity σ . The blue solid curves are the analytical predictions of Pol based on Eq. (12) and Eq. (20), the red circles are Monte Carlo estimations of Pol from Eq. (11) over 100 independent runs of the nonlinear VNM. Parameters are $N = 80$, $K = 3$, with (a) $\eta = 0.1$ and (b) $\eta = 0.3$. The interaction vectors \mathbf{a} are constructed for given values of σ such that $\mathbf{1}^\top \mathbf{h} = 0$, $\|\mathbf{h}\| = \sqrt{N}$.

each simulation, the model is run for 5,000 time-steps and the polarization is computed by averaging the quantity in Eq. (11) over the last 4,000 steps.

In Fig. 2, we investigate the effect of heterogeneity on the polarization by comparing the difference with respect to the heterogeneous VNM. Besides confirming our intuition that heterogeneity hampers coordination, our results suggest that the second-order approximation of the effect of heterogeneity on the polarization is accurate for moderate levels of heterogeneity, that is, up to $\sigma \approx 0.5$.

In Fig. 3, we compare the numerical estimation of the polarization from the simulations and the closed-form approximation, for different levels of the heterogeneity σ , noise η , and average number of interactions K . Our results suggest that the closed-form solution is able to accurately capture the coordination of the heterogeneous VNM up to moderate values of $\eta \approx 0.5$, after which the nonlinear model reaches the completely-discorded state that cannot be predicted by a linear model. The heterogeneity has a secondary role on the extent of the coordination, due to the fact that dependence of the mean-square deviation Eq. (20) with σ^2 is moderated by $K(K-1)^2$ for $N \gg 1$.

V. CONCLUSIONS

In this work, we investigated the effect of heterogeneity on the vectorial network model, a stochastic protocol that is used to examine collective motion of self-propelled particles. By linearizing the dynamics about a synchronous state and leveraging techniques from stochastic consensus and eigenvalue perturbation theories, we established closed-form results for the asymptotic behavior of the model. First, we computed a second-order approximation for the asymptotic convergence factor, which governs the mean-square convergence of the model in the absence of noise. Second, we derived an expression for the polarization of the system, which measures

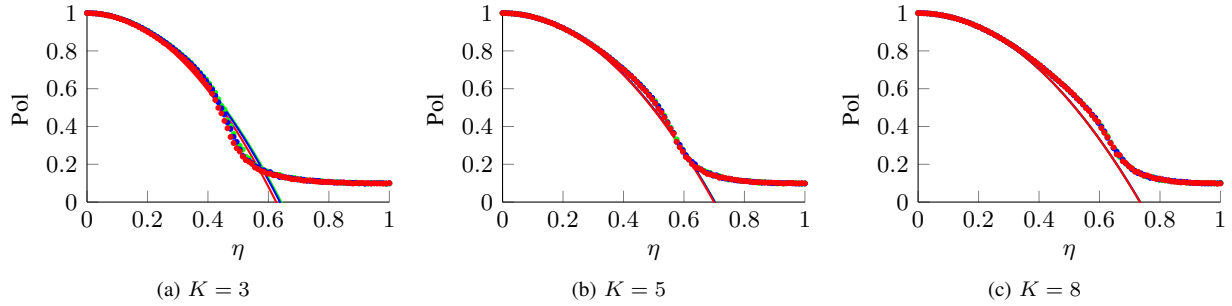


Fig. 3: Polarization for different values of noise η . We consider three different levels of heterogeneity: $\sigma = 0$ (green), $\sigma = 0.5$ (blue), and $\sigma = 1$ (red) and three different average number of interactions (a) $K = 3$, (b) $K = 5$, and (c) $K = 8$. The solid curves are analytical predictions and circles are Monte Carlo estimations over 100 independent runs of the nonlinear VNM. The interaction vectors \mathbf{a} are constructed for given values of σ such that $\mathbf{1}^\top \mathbf{h} = 0$, $\|\mathbf{h}\| = \sqrt{N}$.

the level of coordination between the agents.

Our results support the intuition that heterogeneity has a detrimental effect on collective motion, whereby both the convergence rate and the polarization are reduced as heterogeneity increases. However, the extent of this effect is nonlinearly moderated by the average number of connections made by the agents. From a biological point of view, the robustness of the system to heterogeneity might be a gateway for the emergence of differences in the individual traits of the group that have been shown to beget advantages to life in groups [23]. In linking the predictions of the vectorial network model to more complex self-propelled particle models, future efforts should explore the role of state-dependent stochastic dynamics.

REFERENCES

- [1] D. J. T. Sumpter, *Collective Animal Behavior*, 1st ed. Princeton NJ, US: Princeton University Press, 2010.
- [2] T. Vicsek and A. Zafeiris, "Collective motion," *Phys. Rep.*, vol. 517, no. 3–4, pp. 71–140, 2012.
- [3] F. Bullo, J. Cortes, and S. Martinez, *Distributed Control of Robotic Networks*. Princeton NJ, US: Princeton University Press, 2009.
- [4] M. Aldana, V. Dosiotti, C. Huepe, and H. Larralde, "Phase transitions in systems of self-propelled agents and related network models," *Phys. Rev. Lett.*, vol. 98, no. 9, 2007.
- [5] J. A. Pimentel, M. Aldana, C. Huepe, and H. Larralde, "Intrinsic and extrinsic noise effects on phase transitions of network models with applications to swarming systems," *Phys. Rev. E*, vol. 77, no. 6, 2008.
- [6] T. Vicsek, A. Czirók, E. Ben-Jacob, I. Cohen, and O. Shochet, "Novel type of phase transition in a system of self-driven particles," *Phys. Rev. Lett.*, vol. 75, no. 6, pp. 1226–1229, 1995.
- [7] A. Czirók, E. Stanley, and T. Vicsek, "Spontaneously ordered motion of self-propelled particles," *J. Phys. A*, vol. 30, no. 5, 1997.
- [8] A. Czirók and T. Vicsek, "Collective behavior of interacting self-propelled particles," *Physica A*, vol. 281, no. 1–4, pp. 467–477, 2000.
- [9] G. Grégoire and H. Chaté, "Onset of collective and cohesive motion," *Physica A*, vol. 92, no. 2, 2004.
- [10] A. P. Solon, H. Chaté, and J. Tailleur, "From phase to microphase separation in flocking models: The essential role of nonequilibrium fluctuations," *Phys. Rev. Lett.*, vol. 114, p. 068101, 2015.
- [11] A. Jadbabaie, Jie Lin, and A. S. Morse, "Coordination of groups of mobile autonomous agents using nearest neighbor rules," *IEEE Trans. Autom. Control*, vol. 48, no. 6, pp. 988–1001, 2003.
- [12] A. V. Savkin, "Coordinated collective motion of Groups of autonomous mobile robots: analysis of Vicsek's model," *IEEE Trans. Autom. Control*, vol. 49, no. 6, pp. 981–982, 2004.
- [13] F. Cucker and S. Smale, "Emergent behavior in flocks," *IEEE Trans. Autom. Control*, vol. 52, no. 5, pp. 852–862, 2007.
- [14] G. Tang and L. Guo, "Convergence of a class of multi-agent systems in probabilistic framework," *Journal of Systems Science and Complexity*, vol. 20, no. 2, pp. 173–197, Jun 2007.
- [15] G. Chen, "small noise may diversify collective motion in vicsek model," *IEEE Trans. Autom. Control*.
- [16] M. Porfiri and G. Ariel, "On effective temperature in network models of collective behavior," *Chaos*, vol. 26, no. 4, 2016.
- [17] M. Porfiri, "Linear analysis of the vectorial network model," *IEEE Trans. Circuits Syst., II, Exp. Briefs*, vol. 61, no. 1, pp. 44–48, 2014.
- [18] W. Ren and R. Beard, *Distributed Consensus in Multi-vehicle Cooperative Control*, 1st ed. London, UK: Springer Verlag, 2008.
- [19] A. V. Proskurnikov and R. Tempo, "A tutorial on modeling and analysis of dynamic social networks. Part II," *Ann. Rev. Control*, vol. 45, pp. 166–190, 2018.
- [20] L. Ma, Z. Wang, Q.-L. Han, and Y. Liu, "Consensus control of stochastic multi-agent systems: a survey," *Sci. China. Inform. Sci.*, vol. 60, no. 12, p. 120201, 2017.
- [21] V. Mwaffo and M. Porfiri, "Linear analysis of the vectorial network model in the presence of leaders," *Automatica*, vol. 58, pp. 160–166, 2015.
- [22] V. Mwaffo, R. P. Anderson, and M. Porfiri, "Collective dynamics in the vicsek and vectorial network models beyond uniform additive noise," *J. Nonlinear Sci.*, vol. 25, no. 5, pp. 1053–1076, 2015.
- [23] A. J. King, D. D. Johnson, and M. V. Vugt, "The origins and evolution of leadership," *Curr. Biol.*, vol. 19, no. 19, pp. R911–R916, 2009.
- [24] J. Cortés and M. Egerstedt, "Coordinated control of multi-robot systems: A survey," *SICE J. Control Meas. Syst. Integr.*, vol. 10, no. 6, pp. 495–503, 2017.
- [25] T. Nishikawa, A. E. Motter, Y.-C. Lai, and F. C. Hoppensteadt, "Heterogeneity in oscillator networks: Are smaller worlds easier to synchronize?" *Phys. Rev. Lett.*, vol. 98, no. 1, 2003.
- [26] L. Zino, A. Rizzo, and M. Porfiri, "Consensus over activity driven networks," *IEEE Trans. Control Netw. Syst.*, 2019, (Published Online).
- [27] M. Denker, M. Timme, M. Diesmann, F. Wolf, and T. Geisel, "Breaking synchrony by heterogeneity in complex networks," *Phys. Rev. Lett.*, vol. 92, no. 7, 2004.
- [28] J. Hasanyan, L. Zino, R. Alessandro, and M. Porfiri, "Leader–follower consensus on activity-driven networks," *Proc. R. Soc. A*, vol. 476, no. 2233, 2020.
- [29] S. S. Pereira and A. Pagès-Zamora, "Mean square convergence of consensus algorithms in random WSNs," *IEEE Trans. Signal Process.*, vol. 58, no. 5, 2010.
- [30] S. Patterson, B. Bamieh, and A. El Abbadi, "Convergence rates of distributed average consensus with stochastic link failures," *IEEE Trans. Autom. Control*, vol. 55, no. 4, pp. 880–892, 2010.
- [31] J. Zhou and Q. Wang, "Convergence speed in distributed consensus over dynamically switching random networks," *Automatica*, pp. 1455 – 1461, 2009.
- [32] N. Abaid and M. Porfiri, "Consensus over numerosity-constrained random networks," *IEEE Trans. Autom. Control*, vol. 56, no. 3, pp. 649–654, 2011.
- [33] D. J. Griffiths, *Introduction to Quantum Mechanics*. London, UK: Pearson, 2005.